

Structural and optical properties of Mn-doped CdS thin films prepared by ion implantation

S. Chandramohan, A. Kanjilal, J. K. Tripathi, S. N. Sarangi, R. Sathyamoorthy et al.

Citation: *J. Appl. Phys.* **105**, 123507 (2009); doi: 10.1063/1.3151712

View online: <http://dx.doi.org/10.1063/1.3151712>

View Table of Contents: <http://jap.aip.org/resource/1/JAPIAU/v105/i12>

Published by the [American Institute of Physics](#).

Additional information on J. Appl. Phys.

Journal Homepage: <http://jap.aip.org/>

Journal Information: http://jap.aip.org/about/about_the_journal

Top downloads: http://jap.aip.org/features/most_downloaded

Information for Authors: <http://jap.aip.org/authors>

ADVERTISEMENT



AIP Advances

Now Indexed in Thomson Reuters Databases

Explore AIP's open access journal:

- Rapid publication
- Article-level metrics
- Post-publication rating and commenting

Structural and optical properties of Mn-doped CdS thin films prepared by ion implantation

S. Chandramohan,¹ A. Kanjilal,² J. K. Tripathi,¹ S. N. Sarangi,¹ R. Sathyamoorthy,³ and T. Som^{1,a)}

¹*Institute of Physics, Sachivalaya Marg, Bhubaneswar 751 005, India*

²*Institute for Ion Beam Physics and Materials Research, Forschungszentrum Dresden-Rossendorf, 01328 Dresden, Germany*

³*Department of Physics, Kongunadu Arts and Science College, Coimbatore 641 029, India*

(Received 21 March 2009; accepted 13 May 2009; published online 17 June 2009)

We report on structural and optical properties of Mn-doped CdS thin films prepared by 190 keV Mn-ion implantation at different temperatures. Mn-ion implantation in the fluence range of 1×10^{13} – 1×10^{16} ions cm^{-2} does not lead to the formation of any secondary phase. However, it induces structural disorder, causing a decrease in the optical band gap. This is addressed on the basis of band tailing due to creation of localized energy states and Urbach energy calculations. Mn-doped samples exhibit a new band in their photoluminescence spectra at 2.22 eV, which originates from the d - d (${}^4T_1 \rightarrow {}^6A_1$) transition of tetrahedrally coordinated Mn^{2+} ions. © 2009 American Institute of Physics. [DOI: 10.1063/1.3151712]

I. INTRODUCTION

Cadmium sulfide (CdS) with a direct band gap of 2.42 eV at room temperature (RT) is a useful candidate for solar cells, green lasers, photoconductors, light emitting diodes, and thin film transistors.¹ However, the usefulness of CdS for the futuristic devices resides in the ability to dope it with impurities so as to achieve the desired properties and to make them multifunctional. Recently, there is a growing interest in the synthesis of transition metal (TM) doped CdS nanostructures and thin films due to their anticipated applications in nonvolatile memory and future spintronics devices.^{2,3} The synthesis route employed so far includes sputtering, coevaporation, pulsed laser deposition, and chemical routes.^{2,4}

Alternatively, ion implantation can be considered to be a viable technique for production of doped CdS thin film based planar devices due to its many advantages over the conventional methods, viz. high spatial selectivity, precise control of the impurity concentration, possibility to overcome the solubility limit, and capability of getting seamlessly integrated with different processing steps for manufacturing integrated circuits. However, ion implantation creates lattice disorder, which produces changes in structural, optical, and other physical properties of materials.⁵ Thus, it is important to study such implantation mediated doping induced changes, which would provide useful information to understand the performance of CdS based devices. It can be mentioned that a number of reports exist on ion implantation induced doping of TM elements in CdTe,⁶ ZnO,⁷ GaAs,⁸ GaN,⁹ etc. However, to date, no report is available on the synthesis of TM doped CdS thin films via ion implantation.

In this paper, we report studies on structural and optical properties of Mn-doped CdS thin films prepared by ion implantation. We do not observe any secondary phase forma-

tion. However, implantation induced structural disorder leads to modification in the optical band gap of CdS. We also observe Mn-concentration dependent luminescence from the localized Mn ions in CdS, which can be exploited for flat panel display devices. In addition, we find that CdS is rather radiation-resistant which would be beneficial for its prolonged use in solar cells for space applications, where the devices are continuously exposed to radiation.

II. EXPERIMENTAL

CdS thin films (690 nm thick) were grown on microglass slides at a substrate temperature of 373 K by thermal evaporation. Thickness and composition of the films were measured by Rutherford backscattering spectrometry. Subsequently, the films were implanted with 190 keV Mn ions at RT and at 573 K under identical experimental conditions for a range of Mn-ion fluences starting from 1×10^{13} to 1×10^{16} ions cm^{-2} . These fluences correspond to Mn concentration of 0.0033–3.3 at. % at the peak position of profile. Monte Carlo SRIM2008 simulation¹⁰ predicts the projected range of 190 keV Mn ions in CdS to be 125.2 nm. Phase analysis of the pristine and the Mn-doped CdS films was performed by glancing angle x-ray diffraction (GAXRD) using the Cu-K α radiation ($\lambda=0.154$ nm). The optical transmittance measurements were carried out by using an ultraviolet-visible-near-infrared (UV-visible-NIR) spectrophotometer. Photoluminescence (PL) spectra were recorded at RT with the help of a monochromator in combination with a photomultiplier tube, where a Xe lamp ($\lambda_l=365$ nm) was used as an excitation source.

III. RESULTS AND DISCUSSION

Figure 1 shows the GAXRD patterns recorded at a glancing angle, $\theta_i=1^\circ$ for the pristine and the samples implanted at RT to different fluences. The pristine film is polycrystalline in nature and the observed peak positions match

^{a)}Electronic mail: tsom@iopb.res.in.

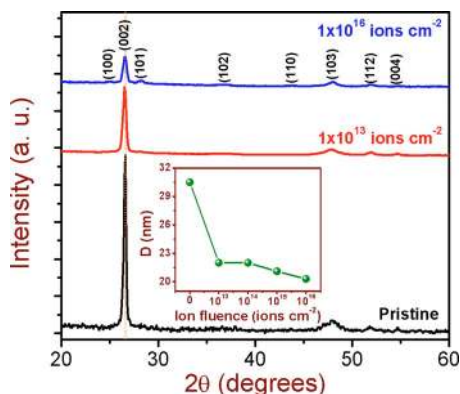


FIG. 1. (Color online) GAXRD patterns of the pristine and the implanted CdS films at RT for typical ion fluences of 1×10^{13} and 1×10^{16} ions cm^{-2} . The inset shows the variation in crystallite size (D) as a function of ion fluence calculated for the predominant (002) peak.

well with the hexagonally close packed, wurtzite structure of CdS with a preferential growth along the (002) direction.¹¹ XRD data reveal that the polycrystalline nature of the films is retained after Mn-ion implantation. In addition, it is observed that although the (002) peak position hardly changes with increasing Mn-ion fluence, the peak intensity decreases. This could happen due to the result of metal-ion doping and/or damage produced during implantation. Moreover, we observe a systematic increase in the full width at half maximum (FWHM) of the (002) peak with increasing ion fluence. According to the theory of kinematical scattering, XRD peaks get broadened either when crystallites become smaller or if lattice defects are present in large enough abundance.¹² The average crystallite size (D) was calculated from the (002) diffraction peaks by using the Scherrer formula ($D = 0.94\lambda/\beta \cos \theta$, where β is the FWHM) and was found to decrease from 31 nm for the undoped sample to a minimum of about 20 nm for the film implanted at the highest fluence of 1×10^{16} ions cm^{-2} at RT (see the inset in Fig. 1). In fact, such an increase in the FWHM and a decrease in the crystallite size due to implantation induced doping have been reported for ZnO as well.⁵ However, we do not observe formation of any metallic clusters or secondary phase precipitates. This could happen due to the supersaturation of implanted ions occupying the substitutional cation sites. Further, the variations in the interplanar spacing d_{002} and the c -axis lattice parameter are found to be extremely small which is quite consistent with those reported for low concentration Mn-doped CdS system.⁴

The band gap energy (E_g) of a direct band gap semiconductor such as CdS can be estimated from the traditional Tauc plot of $(\alpha h\nu)^2$ versus photon energy ($h\nu$), as shown in Fig. 2. The obtained band gap for the pristine CdS film is 2.39 ± 0.01 eV, which decreases down to 2.34 eV following Mn-ion implantation at RT. In general, implanted ions are known to produce a large density of point defects (e.g., vacancies, interstitials, and antisite defects) causing lattice damage. For instance, in our case, SRIM2008 simulation predicts target vacancies of $18 \text{ nm}^{-1} \text{ ion}^{-1}$. These defects can act as trap centers and can affect the optical absorption. In spite of the large density of defects, a marginal decrease in

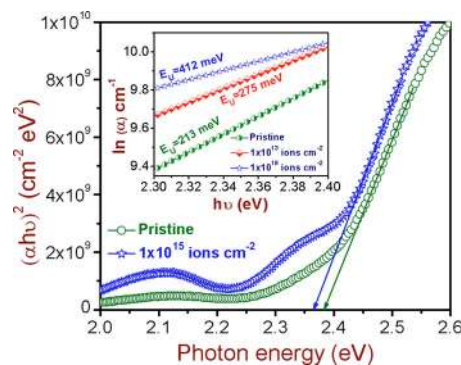


FIG. 2. (Color online) Typical Tauc plot showing change in the optical band gap of CdS films before and after implantation at RT. The inset shows the linear variation in absorption coefficient (α) against photon energy ($h\nu$) in the region $E < E_g$ according to Urbach rule.

the optical band gap indicates that CdS can be considered as a reasonably good radiation-resistant material.

A decrease (marginal though) in the band gap can be associated with defect-induced band tailing due to the creation of localized energy states near the band edges. Earlier studies on ion-implanted CdS films have demonstrated similar occurrence of band gap modification.¹³ We observe a strong absorption below the band edge for the Mn-doped samples, which is attributed to the transitions involving band tails.¹⁴ The width of these band tail states can be well described by the Urbach-tail parameter or Urbach energy (E_U).¹⁴ In our case, since the interference fringes overlap (for low fluences), in order to justify the validity of the subtle change due to implantation induced disorder, the Urbach energy is calculated.

In general, Urbach tails (the exponential variation of absorption coefficient with photon energy below the absorption edge) are considered to be a telltale signature of the presence of different types of impurities, structural disorder, point defects, and grain boundaries in a material.¹⁵ The estimated value of E_U for the pristine CdS film is about 213 meV, which is in good agreement with the value reported in Ref. 16. We observe a systematic increase in E_U with increasing ion fluence (inset of Fig. 2), which could be due to static structural disorder, creating more and more localized states within the band tails of the electronic states. These results substantiate the expected interplay between the structural and the optical properties. We also observe that E_U values for films implanted at 573 K are less than those estimated for films implanted at RT (not shown here). This can be attributed to the fact that implantation at higher temperatures helps in annealing out defects.

Figure 3 shows the normalized PL spectra corresponding to the pristine film and the one implanted at RT to the fluence of 1×10^{15} ions cm^{-2} . The broad nature of the spectra suggests overlapping of different radiative transitions. By using a standard peak fitting process¹⁷ we deconvolute the spectra into different possible bands. In case of the pristine sample, the fitting results into four emission bands centered at 2.286, 2.181, 2.123, and 1.973 eV. The intense green emission band (GB) observed at 2.286 eV is attributed to the radiative transition from localized acceptor states generated by the sulfur

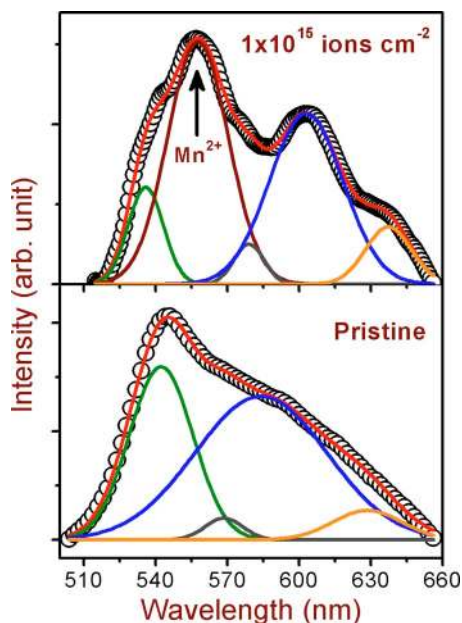


FIG. 3. (Color online) PL spectra of the pristine and the Mn-doped (corresponding to the fluence of 1×10^{15} ions cm^{-2}) CdS films.

interstitials (I_S) to the bottom of the conduction band.¹⁸ The broad band centered at 2.123 eV is known as the yellow emission band (YB) and is associated with radiative transitions from the donor levels, arising due to Cd atoms at the interstitial sites (I_{Cd}), to the valence band.¹⁹ The half width of this band is much broader than the GB, suggesting a high density of interstitial Cd atoms present in the film. We also observe a weak band centered at 1.973 eV, known as orange or red emission band, which can be attributed to complex defects such as $I_{Cd}-V_{Cd}$ Frenkel pairs.¹⁸ These results imply that PL in CdS films is governed by the radiative transitions associated with donor- and acceptor-like shallow levels within the band gap.

The incorporation of Mn-ions into the CdS lattice changes the luminescence properties, as seen from Fig. 3. The GE band located at 2.286 eV (in case of the pristine sample) splits into two bands after Mn-ion implantation regardless of temperature and ion fluence. The new band that emerges around 2.22 eV is a characteristic one for Mn^{2+} related emission, originating from the $d-d$ (${}^4T_1 \rightarrow {}^6A_1$) transition of the tetrahedrally coordinated Mn^{2+} states.^{20,21} Transitions between the ground state (in crystal field notation it is represented by 6A_1) and any of the excited states (4P , 4D , 4F , and 4G , of these, the 4G level has the lowest energy and split into four levels, labeled in group theoretical notation 4T_1 , 4T_2 , 4E , and 4A_1) for free Mn atoms are in principle forbidden by the $\Delta S=0$ and parity selection rules.²² For a Mn^{2+} ion in CdS these selection rules are, respectively, relaxed by the spin-orbit interaction and due to the lack of inversion symmetry of the crystal environment. As a result the $d-d$ transition occurs in our Mn-doped CdS films. We observe a systematic decrease in the amplitude ratio of GB to the Mn-related band and an increase in the FWHM of Mn-related band with increasing ion fluence. This could be probably due to overlapping of ${}^4T_1 \rightarrow {}^6A_1$ and ${}^4T_2 \rightarrow {}^6A_1$ transitions as a result of increase in the Mn content in the sample. This effect

is more prominent for films implanted at 573 K, which suggests that implantation at higher temperature increases the solubility of Mn ions in CdS. Therefore, the implanted Mn ions are likely to occupy the substitutional cation sites in the tetrahedral structure. This corroborates well with our XRD results described earlier. In addition, we observe a decrease in the overall PL intensity due to implantations performed at RT, which could be due to the creation of nonradiative defects. On the other hand, films implanted at 573 K do not show any significant change in the PL intensity, which can be attributed to annealing of radiation-induced defects at higher temperatures. Thus, by choosing the proper implantation parameters, one can control the optical properties of Mn-doped CdS films.

The possible cause for the existence of $d-d$ internal transition of Mn^{2+} can be explained in the light of ion-solid interaction. Based on the electron bombardment experiments performed with 100–300 keV electrons, it has been reported by Kulp²³ that the threshold energy required to knock out the Cd and the S atoms from their lattice positions is 8.7 and 7.3 eV, respectively. In addition, the binding energy of Cd is lesser than that of S. Thus, it is easier to displace a Cd atom than an S atom in the CdS lattice. Monte Carlo SRIM2008 simulation also predicts more displacement of Cd atoms ($9.4 \text{ ion}^{-1} \text{ nm}^{-1}$) than S atoms ($8.7 \text{ ion}^{-1} \text{ nm}^{-1}$) in CdS. Therefore, with increasing ion fluence, Mn ions are likely to occupy the vacancies created by the displaced Cd atoms. However, it is not clear at this point whether the quenching of GB intensity is due to annihilation of number of I_S defects or to any energy transfer process²⁴ between the defect states and the Mn ions.

IV. SUMMARY AND CONCLUSIONS

In summary, we have studied structural and optical properties of Mn-doped CdS thin films prepared by 190 keV Mn^{+} -ion implantation. We do not observe formation of any secondary phase or metallic clustering, which shows the efficacy of this technique for synthesis of TM doped CdS thin films. Mn-doping at RT induces structural disorder, which causes small modification in the optical band gap of CdS by creating localized energy states near the band edges. Thus, CdS can be considered as a reasonably good radiation-resistant material, which can be employed for prolonged use in solar cells for space applications.

A new emission band at 2.22 eV, originating from the $d-d$ transition of the tetrahedrally coordinated Mn^{2+} states, is observed from the Mn-doped samples. The observed Mn-concentration dependent luminescence provides the possibility of incorporating high density of optically active impurity centers in CdS by ion implantation, which can be exploited for application in CdS based flat panel display devices. More experimental investigations are needed to understand whether such high density localized impurities would enhance other properties such as magneto-optical and electroluminescence as well.

¹N. V. Hullavarad, S. S. Hullavarad, and P. C. Karulkar, *J. Nanosci. Nanotechnol.* **8**, 3272 (2008).

²J. C. Lee, N. G. Subramaniam, J. W. Lee, and T. W. Kang, *Appl. Phys.*

- Lett.* **90**, 262909 (2007).
- ³J. S. Kulkarni, O. Kazakova, and J. D. Holmes, *Appl. Phys. A* **85**, 277 (2006).
- ⁴C. T. Tsai, S. H. Chen, and D. S. Chuu, *Phys. Rev. B* **54**, 11555 (1996).
- ⁵A. Mendoza-Galvan, C. Trejo-Cruz, J. Lee, D. Bhattacharyya, J. Metson, P. J. Evans, and U. Pal, *J. Appl. Phys.* **99**, 014306 (2006).
- ⁶D. J. Fu, J. C. Lee, S. W. Choi, C. S. Park, G. N. Panin, T. W. Kang, and X. J. Fan, *Appl. Phys. Lett.* **83**, 2214 (2003).
- ⁷S. Zhou, K. Potzger, J. von Borany, R. Grötzschel, W. Skorupa, M. Helm, and J. Fassbender, *Phys. Rev. B* **77**, 035209 (2008).
- ⁸S. J. Pearton, C. R. Abernathy, D. P. Norton, A. F. Hebard, Y. D. Park, L. A. Boatner, and J. D. Budai, *Mater. Sci. Eng. R.* **40**, 137 (2003).
- ⁹G. Talut, H. Reuther, A. Mücklich, F. Eichhorn, and K. Potzger, *Appl. Phys. Lett.* **89**, 161909 (2006).
- ¹⁰<http://www.srim.org/>
- ¹¹JCPDS Card No. 77-2306.
- ¹²T. Ungar, *Scr. Mater.* **51**, 777 (2004).
- ¹³K. Senthil, D. Mangalaraj, Sa. K. Narayandass, B. Hong, Y. Roh, C. S. Park, and J. Yi, *Semicond. Sci. Technol.* **17**, 97 (2002).
- ¹⁴B. Han, B. W. Wessels, and M. P. Ulmer, *J. Appl. Phys.* **98**, 023513 (2005).
- ¹⁵Z. G. Hu, W. W. Li, J. D. Wu, J. Sun, Q. W. Shu, X. X. Zhong, Z. Q. Zhu, and J. H. Chu, *Appl. Phys. Lett.* **93**, 181910 (2008).
- ¹⁶K. L. Narayanan, K. P. Vijayakumar, K. G. M. Nair, and N. S. Thampi, *Physica B* **240**, 8 (1997).
- ¹⁷Jandel Scientific Peak Fit, Version 2.01, AISN Software, 1990.
- ¹⁸O. Vigil, I. Riech, M. Garcia-Rocha, and O. Zelaya-Angel, *J. Vac. Sci. Technol. A* **15**, 2282 (1997).
- ¹⁹C. Mejia-Garcia, A. Escamilla-Esquivel, G. Contreras-Puente, M. Tufino-Velazquez, M. L. Albor-Aguilera, O. Vigil, and L. Vaillant, *J. Appl. Phys.* **86**, 3171 (1999).
- ²⁰C. W. Na, D. S. Han, D. S. Kim, Y. J. Kang, J. Y. Lee, J. Park, D. K. Oh, K. S. Kim, and D. Kim, *J. Phys. Chem. B* **110**, 6699 (2006).
- ²¹*Diluted Magnetic Semiconductors, Semiconductors and Semimetals*, edited by J. K. Furdyna and J. Kossut (Academic, London, 1988), Vol. 25.
- ²²J. K. Furdyna, *J. Appl. Phys.* **64**, R29 (1988).
- ²³B. A. Kulp, *Phys. Rev.* **125**, 1865 (1962).
- ²⁴R. Beaulac, P. I. Archer, and D. R. Gamelin, *J. Solid State Chem.* **181**, 1582 (2008).